Facial Analysis of Patient Affected by Osteogenesis Imperfecta Using Computer Vision

Rousseau, Maxime
maxime.rousseau2@mail.mcgill.ca

Retrouvey, Jean-Marc
@mcgill.ca

Rauch, Frank
@mcgill.ca

Vargas, Javier
@mcgill.ca

April 14, 2019

1 Abstract

Individuals affected by Osteogenesis Imperfecta (OI), an autosomal dominant genetic disease mainly affecting the COL1A1/A2 genes, have been reported to demonstrate characteristic facial manifestations of the disease. This study uses computer vision and statistical shape analysis to compare the antero-posterior photographs of individuals affected by OI to photographs from a normocephalic control group. Intergroup analysis was also conducted. Facial analysis of subjects affected by Osteogenesis Imperfecta types I, III and IV shows that the facial index is significantly different when compared to controls. Results also point out strong similarities between types I and IV in terms of severity of the facial manifestations and morphology. Previous qualitative literature reports of facial manifestations of OI were validated by our results. Comparison to a baseline shape allowed to pinpoint a typical facial pattern presented by OI individuals. Furthermore, successful classification of patient was performed used logistic regression models.

2 Introduction

Osteogenesis imperfecta is a rare bone disease of genetic etiology. It is autosomal dominant in most cases and mainly affects the COL1A1/A2 genes related to the production of collagen. Other mutations have also been reported (Eimar et al. 2016). The range of phenotypes and severity are wide. Bone fragility is the main issue amongst subjects affected. Subjects often present with a much higher rate of long bone fractures and growth issues (Rauch and Glorieux 2004). Four main types of OI have been described (Chang, Lin, and Hsu 2007) and are based on phenotypes. In order of increasing severity, they are types I, IV, III and II (II being lethal at birth). There is no cure for OI and treatment usually involves the use of IV bisphosphonates (Drake, Clarke, and Khosla 2008). These genetic alterations have craniofacial implications for individuals affected by OI. Only qualitative reports currently address the facial morphology of these patients in the literature. The goal of this study is to explore the facial characteristics of OI types I, III and IV subjects in a quantitative manner and expand on the observations made in the literature. The method leverages computer vision and machine learning to accelerate, standardize and broaden the data gathering effort. A morphological approach relying on a statistical shape methodology was used to conduct our analysis (Ian L. Dryden 2012). We decided that this would be the most accurate method to compare the facial shapes obtained by image processing as it allows for rotation and resizing to summarize a group into a mean shape. Using landmarks also allows us to compute diverse metrics to isolate the differences from an anatomical perspective. The null hypothesis is that there are no statistically significant differences in the facial morphology of subjects affected by different types of OI when compared to normocephalic patients. The authors propose models based on facial landmark which could be considered as a clinical aid to classification and diagnosis to Osteogenesis Im-

perfecta.

3   Study Design

A case-control study was conducted on a total of 306 (M:145/F:161) patients. The Individuals affected by OI where part of the BBDC 7701 study conducted at Shriners Hospital in Montreal, Canada. These patients were grouped according to their OI classification. The first group consisted of 88 (42/46) OI type I subjects. A second group was composed of 28 (9/19) OI type III subjects. The third group consisted of 57 (26/31) OI type IV subjects. The control group consisted of 133 (68/65) patients (Figure 1). Population testing for sex (Chi-Squared) and age (ANOVA) showed no statistically significant difference between the groups (Table 1). The selection criteria for the control group was to present a facial index 0.80 which is considered as the ideal facial proportions between height and width of the face (Franco et al. 2013). The measurement is a ratio of face height by the bizygomatic width. This index was preferred for the control group as it is deemed preferable to have a uniform control group to identify the facial characteristics of OI subjects. Having a static baseline would allow us to better isolate the discrepancies presented by patients affected by OI.
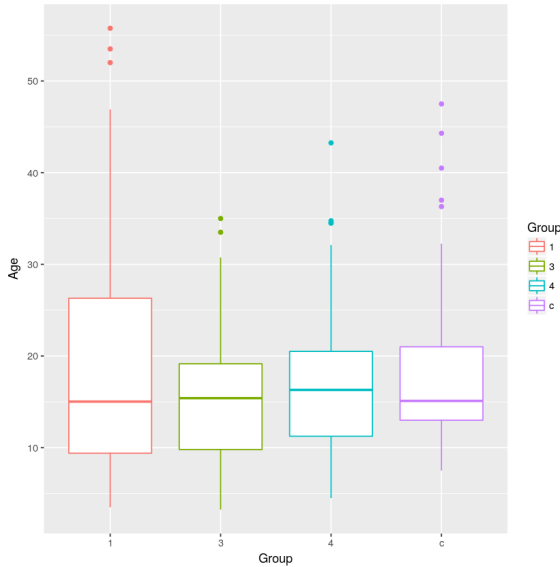
4   Materials and Methods

Antero-posterior photographs of the subjects' faces were used for this analysis. These pictures where all taken by the same operator using a Canon D 70 Dental Eye camera following the McGill University photography protocol. Pictures that did not meet the requirements for a proper extra-oral orthodontic photograph were excluded from the study. The python and R notebooks used in this study were published on GitHub. This study makes use of the OpenCV (Itseez 2017) open source computer vision library, the Dlib library and a publicly available facial annotation tool (Sagonas et al. 2013). The machine learning models were written with the Scikit Learn library. This program detected the patients faces through a process called a Haar cascade (Viola and Jones 2001). After having fitted the face to a rectangle, 68 landmarks were automatically identified on each facial photograph (Figure 1). The algorithm placing the landmarks was pre-trained on 300 sample faces. X, Y coordinates from these landmarks were stored in matrices for use in our statistical analysis.
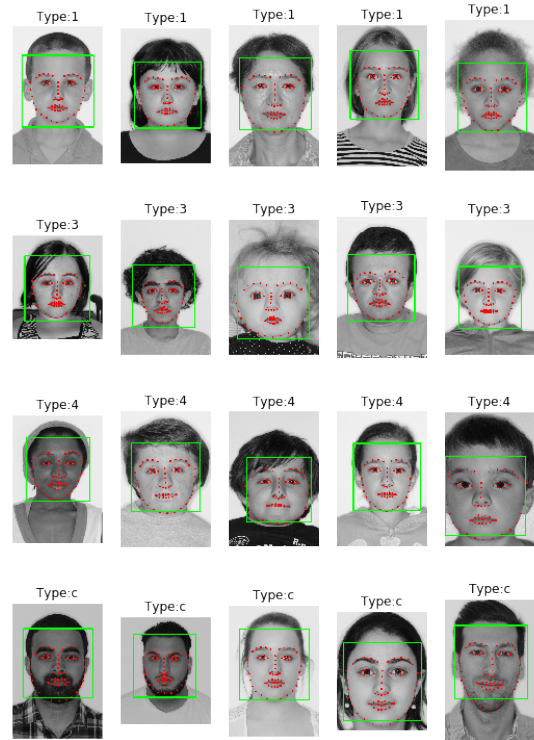

Figure 1: Population sample ages

Figure 2: Face Detection and Landmark Placement

To be able to compare the landmarks further manipulations were done using the R statistical programming language as well as the Shapes package (Dryden 2017). The landmark data of each groups was then processed using Generalized Procrustes Analysis (GPA). This algorithm scaled and rotated the shapes within a group for optimal fit then computed the mean shape for the group. A new group landmark dataset was saved using the rotated and scaled landmark coordinates. This dataset was then used to compute all our metrics for statistical analysis and train classifiers.

The mean shapes were used for the comparison of the affected groups to the control group. An intergroup analysis was also conducted. These comparisons were computed with Goodall's F-Test for statistical significance. Using the mean shape of the control group as a baseline, the distance of each landmark from the baseline coordinates were also computed for each patient. This distance was calculated using Euclidean geometry to get an absolute value. The results were compiled as mean distances per landmark for each group to detect the differences in the morphologies of the OI types. The population mean value was set using the control group. Three facial ratios and the lower face height (LFH) of each patient were also computed for each patient using the same set of landmarks coordinates (Figure 3). Z-scores were computed for each metric. The groups were tested using ANOVA with Bonferroni post-hoc tests (table 1).

(a)

$$MED = \frac{\sum_{n=1}^{68} \sqrt{(b_i^x - l_i^x)^2 + (b_i^y - l_i^y)^2}}{68}$$

(b)

$$R_1 = (l_{46} - l_{37})/(l_{17} - l_1)$$

(c)

$$R_2 = (l_{13} - l_5)/(l_{17} - l_1)$$

(d)

$$R_3 = (l_{17} - l_1)/(l_{28} - l_9)$$

(e)

$$LFH = (l_{34} - l_9)/(l_{28} - l_9)$$

Figure 3: Equations of the measurements taken from the samples for our statistical analysis
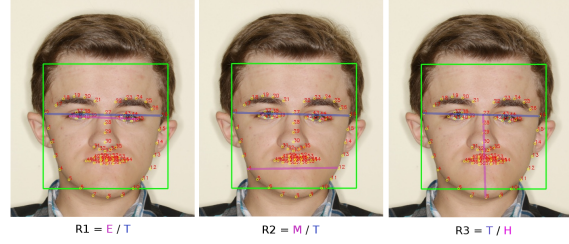

Figure 4: Facial Ratios Used for Facial Analysis

Three different classifiers were trained, all of which had the same architecture. The input layer consisted of 138 features. 68 x and y coordinates as well as the age and sex of the patient. Principal component analysis was used to reduce the dimension to 30 features which were then passed through a logistic regression (Figure 4). The train/test set were created from an 80/20 split of the dataset. Two binary classifiers were trained as well as one multiclass classifier. The first binary classifier was used to classify controls and OI type I patient as these are sometimes hard to distinguish clinically. The second one, was had to detect whether the patient was affected by OI (all types included). The multiclass model had to detect whether the patient was a control, OI type I/IV or OI type III.
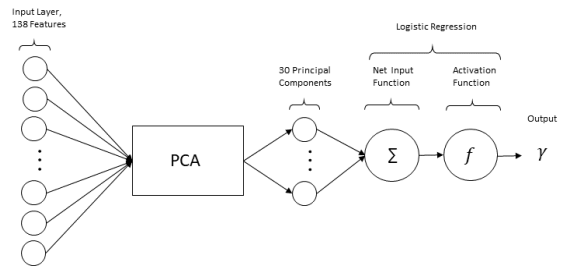

Figure 5: Schematic Representation of Classifiers

5   Results

The p-values obtained from the mean shape comparison of the groups were all statistically significant except for the comparison between subjects affected by type I OI to those affected by type IV.

3

	Control	OI Type I	OI Type III	OI Type IV	P-Value
N (M/F)	133(68/65)	88(42/46)	28(9/19)	57(26/31)	P(Chi-Squared) = 0.32
Age (years)	17.7(7.7)	19.7(14)	15.4(8.4)	17.1(8.4)	P(ANOVA) = 0.19
MED	NA	$0.0075^{bc}(0.005)$	$0.0106^{c}(0.008)$	$0.0081(0.006)$	P(ANOVA) < 0.05
MED Z-Score	NA	$-0.122^{bc}(0.907)$	$0.439^{c}(1.156)$	$-0.027(0.995)$	P(ANOVA) < 0.05
Ratio 1	$0.612^{a}(0.026)$	$0.595(0.026)$	$0.604(0.036)$	$0.602(0.031)$	P(ANOVA) < 0.05
Ratio 1 Z-Score	$0.246^{a}(0.901)$	$-0.323(0.926)$	$0.008(1.242)$	$-0.080(1.069)$	P(ANOVA) < 0.05
Ratio 2	$0.799^{a}(0.027)$	$0.784(0.038)$	$0.774(0.030)$	$0.791(0.031)$	P(ANOVA) < 0.05
Ratio 2 Z-Score	$0.247^{a}(0.839)$	$-0.215(1.175)$	$-0.537(0.912)$	$0.021(0.944)$	P(ANOVA) < 0.05
Ratio 3	$1.26^{abc}(0.075)$	$1.33^{b}(0.106)$	$1.40^{c}(0.124)$	$1.33(0.097)$	P(ANOVA) < 0.05
Ratio 3 Z-Score	$-0.444^{abc}(0.726)$	$0.264^{b}(1.02)$	$0.909^{c}(1.191)$	$0.181(0.938)$	P(ANOVA) < 0.05
LFH	$0.569(0.022)$	$0.571(0.027)$	$0.562(0.035)$	$0.567(0.026)$	P(ANOVA) = 0.47
LFH Z-Score	$0.0185(0.871)$	$0.0818(1.02)$	$-0.253(1.407)$	$-0.045(1.021)$	P(ANOVA) = 0.47

Table 1: Results from the Measurements and Statistical Testing. a: $p < 0.05$ in comparison to OI-I b: $p < 0.05$ in comparison to OI-III c: $p < 0.05$ in comparison to OI-IV

The results of our other analyses are summarized in Table 1.

The accuracy metrics for the different models are summarized in table 2. We can see the confusion matrices of the models in figure 5.

Model	Class	Precision	Recall	F1-Score	Support
OIM0	Control	1.00	1.00	1.00	27
	OI Type 1 + 4	0.97	1.00	0.98	29
	OI Type 3	1.00	0.80	0.89	5
	Total	0.98	0.98	0.98	61
OIB0	Control	1.00	1.00	1.00	26
	OI Type 1	1.00	1.00	1.00	18
	Total	1.00	1.00	1.00	44
OIB1	Control	1.00	1.00	1.00	25
	OI Subject	1.00	1.00	1.00	36
	Total	1.00	1.00	1.00	61

Table 2: Accuracy Metrics from the Classifiers Test Set

6 Discussion

Considering the body of results obtained, the null hypothesis is rejects. This confirms previous literature reports of a different facial morphology for the patients affected by OI. Mean shape testing seems to be more robust at detecting morphological differences in between the group though it provides us with less insight. However, by visualizing the results for the MED (Figure 6) we can see that the landmark situated at the temples (1 and 17) and the lateral edges of the eyes (27 and 46) account for much of the discrepancies that are observed. This seems to be related to the tri-angular facial morphology described in previous articles. CBCT imaging had also revealed prominent temporal bones in patients affected by OI. When looking at the other metrics computed to assess the facial characteristics of the patients we see that the ones involving the bitemporal width will show statistically significant results. On the other hand, the LFH measurement which only takes the vertical aspect of the face into account was the only metric that showed no intergroup differences. Also, similarly to the mean shape test, the MED metric seem to be more reliable when comparing the facial morphology of the subjects than any other single measurement taken. It is also intuitive that a method which encompasses more landmarks enables for a more accurate analysis. The ability to train successful classifiers using landmarks and general patient data as input features also opens the door to potential diagnostics aids. Given that OI is a rare disease the main limitation to the sophistication of the models is the size of the dataset. However, simple models can still be an effective diagnostic aid for clinicians lacking an expertise in rare genetic bone disease.

7 Conclusions

Our results confirm the previous reports in the literature reporting specific facial characteristics in subjects affected by Osteogenesis Imperfecta. Our analysis also suggests that these manifestations are present to varying degrees depending on the classification of the disease and that type III

group is the more severely affected. The different facial analysis ran on these patients seem to point to deformities at the level of the temples jaw and facial height relative to the patient's general morphology. The findings of this study indicate potential issues in the phenotypic classification initially put forth by Sillence. The strong similarities between the patient from the type I and type IV groups challenge our current understanding of the facial manifestations of the disease. The findings of this study give us new insight as to where to look for discrepancies with normal patients when it comes to the facial characteristics of individuals affected by Osteogenesis Imperfecta. The next step will be to determine the extent of these differences and devise method to identify the severity of the disease through automated facial recognition software.

8 References

Chang, P. C., S. Y. Lin, and K. H. Hsu. 2007. 'The craniofacial characteristics of osteogenesis imperfecta patients', *European Journal of Orthodontics*, 29: 232-7.

Drake, M. T., B. L. Clarke, and S. Khosla. 2008. 'Bisphosphonates: mechanism of action and role in clinical practice', *Mayo Clinic Proceedings*, 83: 1032-45.

Dryden, I. L. 2017. "shapes package." In. Vienna, Austria: R Foundation for Statistical Computing.

Eimar, H., F. Tamimi, J. M. Retrouvey, F. Rauch, J. E. Aubin, and M. D. McKee. 2016. 'Craniofacial and Dental Defects in the Col1a1Jrt/+ Mouse Model of Osteogenesis Imperfecta', *Journal of Dental Research*, 95: 761-8.

Franco, F. C., T. M. de Araujo, C. J. Vogel, and C. C. Quintao. 2013. 'Brachycephalic, dolichocephalic and mesocephalic: Is it appropriate to describe the face using skull patterns?', *Dental Press J Orthod*, 18: 159-63.

Ian L. Dryden, Kanti V. Mardia. 2012. *Statistical Shape Analysis: With Applications in R* (John Wiley \& Sons).

Itseez. 2017. "Open Source Computer Vision Library." In.: \url{https://github.com/itseez/opencv}.

Rauch, F., and F. H. Glorieux. 2004. 'Osteogenesis imperfecta', *Lancet*, 363: 1377-85.

Sagonas, C., G. Tzimiropoulos, S. Zafeiriou, and M. Pantic. 2013. 'A Semi-automatic Methodology for Facial Landmark Annotation': 896-903.

Viola, P., and M. Jones. 2001. "Rapid object detection using a boosted cascade of simple features." In *Proceedings of the 2001 IEEE Computer Society Conference on Computer Vision and Pattern Recognition. CVPR 2001*, I-I.
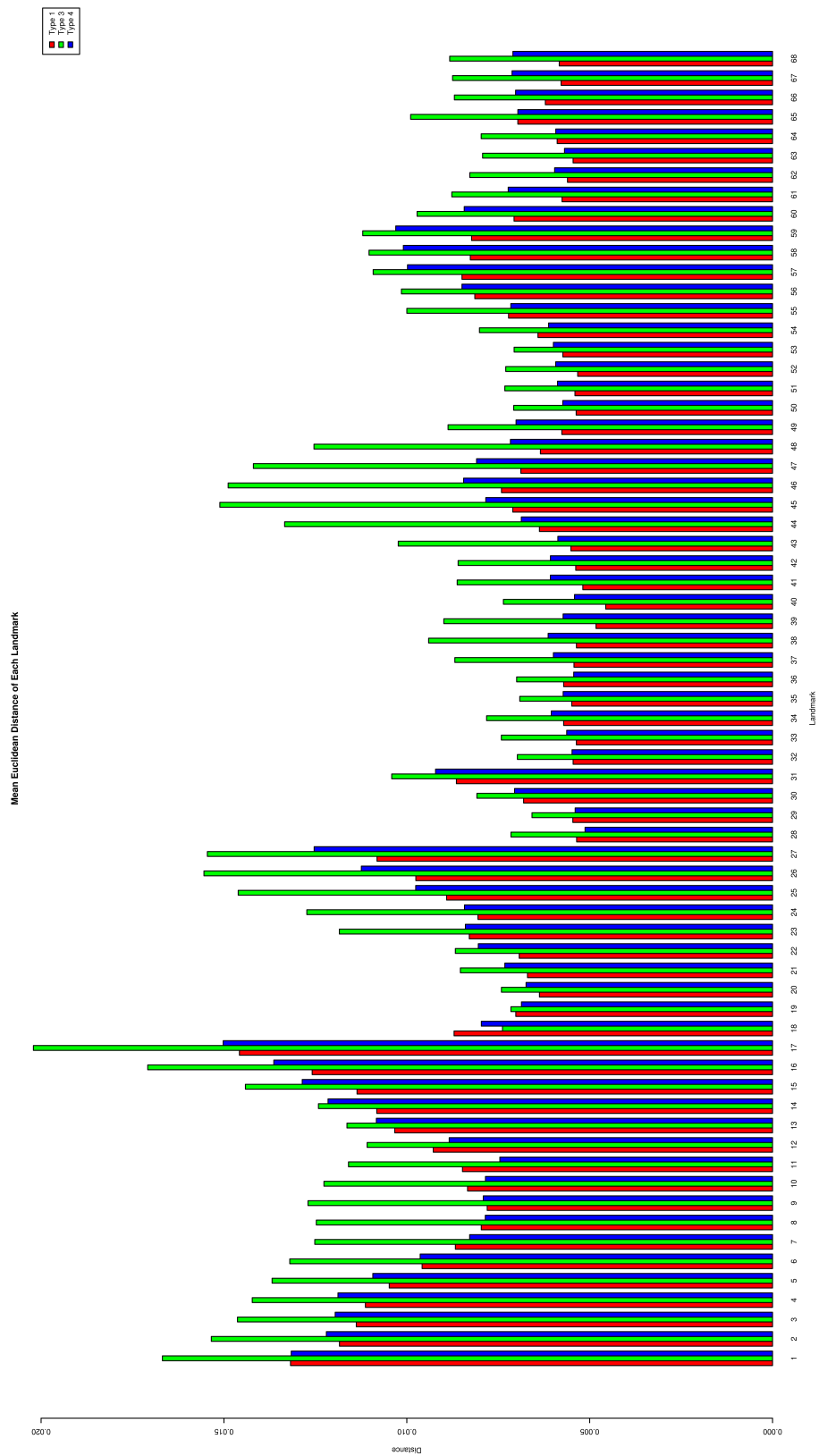
A Additional Figures

Figure 6: Histogram of the MED of OI Groups